

# On the gluon shadowing effect in light and heavy nuclei at small $x$

A.V. Lipatov<sup>1</sup>, G.I. Lykasov<sup>2</sup>, M.A. Malyshev<sup>1,3</sup>

May 6, 2025

<sup>1</sup>*Skobeltsyn Institute of Nuclear Physics, Lomonosov Moscow State University, 119991 Moscow, Russia*

<sup>2</sup>*Joint Institute for Nuclear Research, 141980 Dubna, Moscow region, Russia*

<sup>3</sup>*Moscow Aviation Institute, 125993 Moscow, Russia*

## Abstract

We propose new Transverse Momentum Dependent (TMD) gluon densities in nuclei. Our method is based on a combination of the color dipole scattering formalism, within which we interpret the nuclear deep inelastic structure functions  $F_2^A(x, Q^2)$  and well established property of geometrical scaling from nucleons to nuclei. As an input, we employ the TMD gluon density in a proton which provides a self-consistent simultaneous description of the numerous HERA and LHC data on  $pp$ ,  $ep$  and  $\gamma p$  processes. After fitting the relevant phenomenological parameters to the experimental data on the ratios  $F_2^A(x, Q^2)/F_2^{A'}(x, Q^2)$  for several nuclear targets  $A$  and  $A'$ , we derive the corresponding nuclear gluon distributions. Then, we make predictions for gluon shadowing effects at small Bjorken  $x$  in their dependence of the mass number  $A$ . A comparison with other approaches is given.

*Keywords:* small- $x$  physics, TMD gluon density in a proton and nuclei, deep inelastic scattering, color dipole approach, nuclear gluon shadowing and anti-shadowing

It is well known that a significant effect of nucleon interaction in the nucleus appears in the deep inelastic scattering (DIS) of leptons on nuclei. It demolishes the naive idea of the nucleus as a system of quasi-free nucleons [1–4]. However, the standard concept of QCD factorization for  $ep$  or  $pp$  collisions, where cross sections of arbitrary hard production processes are calculated as a convolution of short-distance partonic cross sections and parton (quark or gluon) distribution functions in a proton (PDFs), is often extrapolated to  $eA$  and  $pA$  interactions. In this case, proton PDFs are replaced by nuclear PDFs (nPDFs) with keeping hard scattering cross sections the same [5–7]. Therefore, detailed knowledge of nPDFs, in particular, the gluon distribution in nuclei, is necessary for theoretical description of the interaction dynamics in  $eA$ ,  $pA$  and  $AA$  processes studied at modern (LHC, RHIC) and future colliders (FCC-he, EIC, EicC, CEPC, NICA).

Influence of nuclear effects on PDFs meets a lot of interest from both theoretical and experimental points of view. Usually the nuclear modification factor, defined as a ratio of per-nucleon structure functions in nuclei  $A$  and deuteron<sup>1</sup>  $R = F_2^A(x, Q^2)/F_2^D(x, Q^2)$ , is introduced and its behaviour in the different  $x$  ranges is investigated. So, there are shadowing, anti-shadowing, valence quarks and Fermi motion dominance regions at  $x \leq 0.1$ ,  $0.1 \leq x \leq 0.3$ ,  $0.3 \leq x \leq 0.7$  and  $x \geq 0.7$ , respectively. The shadowing and anti-shadowing effects refer to  $R < 1$  and  $R > 1$  values, whereas EMC effect and Fermi motion refer to the slope of  $R$  in the valence-dominant region and rising of  $R$  at larger  $x$ . Different mechanisms are responsible for the different nuclear effects. Unfortunately, up to now there is no commonly accepted framework to describe the nuclear modification of PDFs in the whole kinematical range. Two main approaches are used by different groups. In the first of them, nPDFs are extracted from a global fit to nuclear data and their scale dependence is governed then by standard Dokshitzer-Gribov-Lipatov-Altarelli-Parisi (DGLAP) equations (see [5–8]). The second strategy is based on special nPDF models (see, for example, [9, 10] and references therein). Nevertheless, quark and especially gluon distributions in nuclei still have large uncertainties in the whole  $x$  region due to shortage of experimental data and/or limited kinematic coverage of the latter [11–13].

Nowadays, approaches based on the Transverse Momentum Dependent (TMD) parton densities<sup>2</sup> have become quite popular in phenomenological analyses of QCD processes (see, for example, reviews [17, 18] for more information). In this Letter we investigate applicability of a model [19, 20] to the lepton-nucleus ( $eA$ ) collisions. Our study is inspired by the self-consistent simultaneous description of numerous HERA and LHC data (in particular, data on the proton structure function  $F_2(x, Q^2)$ , reduced cross sections  $\sigma_r(x, Q^2)$  for the electron-proton deep inelastic scattering at HERA and soft hadron production in  $pp$  collisions at LHC) achieved within this model. Using the well established property of geometrical scaling [21] and an ansatz [22], we extend the proposed gluon density to nuclei and study the structure function ratio between various nuclei at low  $x$  within the color dipole approach. Such quantities are known to be a powerful tool to investigate the nuclear and nucleon structure. Performing a fit on available experimental data [23–34], we derive nuclear TMD gluon densities (nTMDs) at low  $x$  ( $x \leq 0.1$ ) for several nuclei targets and then investigate corresponding shadowing effects with respect to the mass number  $A$ . The consideration below continues the line of our studies [19, 20, 35–37]. Similar calculations were done earlier [22, 38]. However, these calculations based on the popular Golec-Biernat-Wüsthoff (GBW) model [39, 40], which have some known difficul-

<sup>1</sup>Or rather ratio of corresponding parton densities.

<sup>2</sup>The TMD parton densities are widely used in the Collins-Soper-Sterman approach [14] designed for semi-inclusive processes with a finite and non-zero ratio between the hard scale  $\mu^2$  and total center-of-mass energy  $\sqrt{s}$ . In the High Energy Factorization [15], or  $k_T$ -factorization [16] approach, developed for high energy hadronic collisions proceeding with a large momentum transfer and involving several hard scales, the TMD parton densities are often referred as unintegrated parton distributions (uPDFs).

ties in description of data (see, for example, [41]). This is in a clear contrast with our input [19, 20].

For the reader's convenience, first we recall some important formulas. So, in the color dipole formalism [42–46] the cross section of scattering between the transversely ( $T$ ) and longitudinally ( $L$ ) polarized virtual photons  $\gamma^*$  and proton or nucleus  $A$  at small  $x$  reads

$$\sigma_{T,L}^{\gamma^*h}(x, Q^2) = \int d^2\mathbf{r} \int_0^1 dz |\Psi_{T,L}^{\gamma^*}(z, r, Q^2)|^2 \hat{\sigma}^h(x, r^2), \quad (1)$$

where the total cross section  $\sigma^{\gamma^*h}(x, Q^2) = \sigma_T^{\gamma^*h}(x, Q^2) + \sigma_L^{\gamma^*h}(x, Q^2)$  with  $h = p$  or  $A$ ,  $\Psi_{T,L}^{\gamma^*}(z, r, Q^2)$  are the transverse and longitudinal spin-averaged perturbatively calculated wave functions [44] for the splitting of a photon  $\gamma^*$  having virtuality  $Q^2$  into a dipole  $q\bar{q}$  with transverse size  $r$ ,  $z$  is the quark longitudinal momentum fraction with respect to the photon momentum  $q$  (and  $1 - z$  for antiquark),  $x = Q^2/(W^2 + Q^2)$ ,  $Q^2 = -q^2$ ,  $W^2 = (p + q)^2$  with  $p$  being the proton or nucleus momentum. The squared photon wave functions read

$$|\Psi_T^{\gamma^*}(z, r, Q^2)|^2 = \frac{6\alpha}{4\pi^2} \sum_f e_f^2 \{ [z^2 + (1 - z)^2] \epsilon^2 K_1^2(\epsilon r) + m_f^2 K_0^2(\epsilon r) \},$$

$$|\Psi_L^{\gamma^*}(z, r, Q^2)|^2 = \frac{6\alpha}{4\pi^2} \sum_f e_f^2 \{ 4Q^2 z^2 (1 - z)^2 K_0^2(\epsilon r) \}, \quad (2)$$

where  $\epsilon^2 = z(1 - z)Q^2 + m_f^2$ ,  $K_0$  and  $K_1$  are McDonald functions and summation is performed over the quark flavors  $f$ . The dipole cross section  $\hat{\sigma}^h(x, r^2)$  contains all information about the target  $h$  and hard interaction. It is very difficult to calculate  $\hat{\sigma}^h(x, r^2)$  *ab initio* and, therefore, usually it is modelled (see, for example, [39, 40, 47] and references therein). In the case of proton, the dipole cross section  $\hat{\sigma}^p(x, r^2)$  within the GBW approach was proposed in the form [39, 40]

$$\hat{\sigma}^p(x, r^2) = \sigma_0 \left\{ 1 - \exp \left[ -\frac{r^2}{R_0^2(x)} \right] \right\}, \quad R_0^2(x) = \frac{1}{Q_0^2} \left( \frac{x}{x_0} \right)^\lambda, \quad (3)$$

where  $\sigma_0$ ,  $Q_0$ ,  $x_0$  and  $\lambda$  are free parameters and gluon saturation [39, 40, 43] at small  $x$  (see also [48]) is taken into account. In the improved (BGK) model,  $\hat{\sigma}^p(x, r^2)$  at large enough  $\mu^2$  reads [47]

$$\hat{\sigma}^p(x, r^2) = \sigma_0 \left\{ 1 - \exp \left[ -\frac{\pi^2 r^2 \alpha_s(\mu_r^2) x g(x, \mu_r^2)}{3\sigma_0} \right] \right\}, \quad (4)$$

where  $xg(x, \mu_r^2)$  is the gluon distribution function,  $\mu_r^2 = C/r^2 + \mu_0^2$  with  $C$  and  $\mu_0^2$  being fitted to the experimental data. In the leading  $\ln 1/x$  limit, which corresponds to the approximation of two gluon exchange between the color dipole  $q\bar{q}$  and proton debris, there is a relation between the gluon distribution function in a proton and dipole cross section:

$$\hat{\sigma}^p(x, r^2) = \frac{4\pi^2 \alpha_s}{3} \int \frac{d\mathbf{k}_T^2}{\mathbf{k}_T^2} [1 - J_0(|\mathbf{k}_T| r)] f_g^p(x, \mathbf{k}_T^2), \quad (5)$$

where  $J_0$  is the Bessel function of zeroth order and  $\alpha_s$  is the fixed QCD coupling. The gluon density  $f_g^p(x, \mathbf{k}_T^2)$  depends on the transverse momentum  $\mathbf{k}_T^2$  and is therefore called TMD (or unintegrated) one. So, from expressions (3) and (5) one can immediately obtain

$$f_g^p(x, \mathbf{k}_T^2) = \frac{3\sigma_0}{4\pi^2} R_0^2(x) \mathbf{k}_T^2 \exp [-R_0^2(x) \mathbf{k}_T^2]. \quad (6)$$

It is important that the so-called  $x$ -dependent saturation radius  $R_0(x)$  involved into (3) and (6) determines the corresponding saturation scale  $Q_s(x) = 1/R_0(x)$ . The latter regulates the partial saturation dynamics of gluon densities at scales less than  $Q_s(x)$ :  $f_g^p(x, \mathbf{k}_T^2) \simeq \text{const} \times \ln 1/x$  [39, 40, 43].

In our previous paper [19] the TMD gluon density in a proton at low scale  $\mu^2 \simeq Q_0^2$  was proposed in another form (LLM):

$$f_g^p(x, \mathbf{k}_T^2) = c_g(1-x)^{b_g} \sum_{n=1}^3 c_n (R_0(x)|\mathbf{k}_T|)^n \exp(-R_0(x)|\mathbf{k}_T|),$$

$$b_g = b_g(0) + \frac{4C_A}{\beta_0} \ln \frac{\alpha_s(Q_0^2)}{\alpha_s(\mathbf{k}_T^2)}, \quad (7)$$

where  $C_A = N_c$ ,  $\beta_0 = 11 - 2/3N_f$  and  $Q_0 = 2.2$  GeV. All phenomenological parameters, namely,  $c_g$ ,  $x_0$ ,  $\lambda$ ,  $b_g(0)$  and  $c_n$  were determined [19, 20, 37] from a fit to numerous HERA and LHC data for processes extremely sensitive to the gluon content of a proton. In particular, gluon density (7) provides a self-consistent simultaneous description of the HERA data on the proton structure function  $F_2(x, Q^2)$ , reduced cross section  $\sigma_r(x, Q^2)$  for the electron-proton deep inelastic scattering at low  $Q^2$  and soft hadron production in  $pp$  collisions at the LHC conditions<sup>3</sup>. Dynamics of the gluon saturation predicted by (7) was specially investigated [19, 37]. So, it was shown that expression (7) leads to a smaller  $Q_s$  than the GBW model at the same  $x$ .

An essential point of our derivation below is the so-called geometric scaling [21], which is a characteristic feature of low- $x$  data on the deep inelastic lepton-proton scattering at HERA. In fact, the data on  $\sigma^{\gamma^*p}(x, Q^2)$  cross section over a wide range of  $Q^2$  can be described<sup>4</sup> by a single variable  $\tau = Q^2/Q_s^2(x)$ , where all  $x$  dependence is encoded in the saturation scale  $Q_s^2(x) \sim x^{-\lambda}$  with  $\lambda \sim 0.3$ . The same scaling effect was observed for nuclear cross sections  $\sigma^{\gamma^*A}(x, Q^2)$  [22]. It was shown that

$$\frac{\sigma^{\gamma^*A}(\tau)}{\pi R_A^2} = \frac{\sigma^{\gamma^*p}(\tau)}{\pi R_p^2}, \quad (8)$$

where  $R_h$  is the radius of the hadronic target and  $\tau = \tau_A \equiv Q^2/Q_{s,A}^2$  or  $\tau = \tau_p \equiv Q^2/Q_s^2$ , respectively. So, the  $A$ -dependence of the ratio  $\sigma^{\gamma^*h}(x, Q^2)/\pi R_h^2$  can be absorbed in the  $A$ -dependence of  $Q_{s,A}(x)$ . For this dependence, an ansatz was proposed [22]:

$$Q_{s,A}^2(x) = Q_s^2(x) \left( \frac{A\pi R_p^2}{\pi R_A^2} \right)^{\frac{1}{\delta}} \quad (9)$$

where  $\delta$  and  $\pi R_p^2$  are free parameters. The nuclear gluon distribution could be obtained from the gluon density in a proton after replacement  $Q_s^2(x) \rightarrow Q_{s,A}^2(x)$  [22] and applying the overall normalization factor  $R_A^2/R_p^2$ , which immediately comes from (8).

Now we can extend the gluon density (7) to the nuclei and investigate structure function ratios between various nuclei and/or deuteron. As usual, these structure functions,  $F_2^h(x, Q^2)$ , are calculated as the sum of the transverse and longitudinal ones:

$$F_2^h(x, Q^2) = F_T^h(x, Q^2) + F_L^h(x, Q^2), \quad (10)$$

<sup>3</sup>Being evolved according to the Catani-Ciafaloni-Fiorani-Marchesini equation [49], the gluon density (7) provides good description of the LHC data on heavy flavor and Higgs production at different energies, HERA data on the prompt photon production, proton structure functions  $F_2^c(x, Q^2)$ ,  $F_2^b(x, Q^2)$  and longitudinal structure function  $F_L(x, Q^2)$  in a wide range of  $x$  and  $Q^2$  [19, 20, 35–37].

<sup>4</sup>The geometric scaling naturally arises in the non-linear small- $x$  QCD evolution equations. See, for example, [50–53].

Targets	Experiment	Reference	Number of data points
$^4\text{He}/\text{D}$	NMC	[28]	11
$^6\text{Li}/\text{D}$	NMC	[29]	17
$^{12}\text{C}/\text{D}$	NMC	[28]	11
$^{12}\text{C}/\text{D}$	NMC	[29]	17
$^{12}\text{C}/\text{D}$	EMC	[23]	3
$^{12}\text{C}/\text{D}$	EMC	[24]	15
$^{12}\text{C}/\text{D}$	EMC	[25]	9
$^{12}\text{C}/\text{D}$	E665	[34]	10
$^{40}\text{Ca}/\text{D}$	EMC	[24]	15
$^{40}\text{Ca}/\text{D}$	EMC	[25]	9
$^{40}\text{Ca}/\text{D}$	NMC	[28]	11
$^{40}\text{Ca}/\text{D}$	E665	[34]	10
$^{56}\text{Fe}/\text{D}$	SLAC	[32]	1
$^{64}\text{Cu}/\text{D}$	EMC	[23]	3
$^{64}\text{Cu}/\text{D}$	EMC	[26]	4
$^{119}\text{Sn}/\text{D}$	EMC	[23]	3
$^{131}\text{Xe}/\text{D}$	E665	[33]	9
$^{208}\text{Pb}/\text{D}$	EMC	[34]	10
$^{12}\text{C}/^6\text{Li}$	NMC	[27]	17
$^{12}\text{C}/^6\text{Li}$	NMC	[28]	17
$^{40}\text{Ca}/^6\text{Li}$	NMC	[27]	8
$^{40}\text{Ca}/^6\text{Li}$	NMC	[28]	8
$^9\text{Be}/^{12}\text{C}$	NMC	[30]	8
$^{27}\text{Al}/^{12}\text{C}$	NMC	[30]	8
$^{40}\text{Ca}/^{12}\text{C}$	NMC	[30]	8
$^{56}\text{Fe}/^{12}\text{C}$	NMC	[30]	8
$^{208}\text{Pb}/^{12}\text{C}$	NMC	[30]	8
$^{119}\text{Sn}/^{12}\text{C}$	NMC	[30]	8
$^{119}\text{Sn}/^{12}\text{C}$	NMC	[31]	83

Table 1: List of nuclear data used in our fit. Number of data points at  $x < 0.1$  are shown in last column.

where  $F_T^h(x, Q^2)$  and  $F_L^h(x, Q^2)$  can be obtained within the color dipole approach at low  $x$  using (1) — (5) as:

$$F_{T,L}^h(x, Q^2) = \frac{Q^2}{4\pi^2\alpha} \sigma_{T,L}^{\gamma^*h}(x, Q^2). \quad (11)$$

The formulae listed above allow us to calculate the structure functions  $F_2^A(x, Q^2)$  for various nuclei. As mentioned above, the scaling parameters  $\pi R_p^2$  and  $\delta$  are to be fitted from data. Since we are interested in the low  $x$  region, where shadowing takes place and gluon distribution contributes dominantly, we have performed such a fit on structure function ratio data taken at  $x < 0.1$  by the EMC [23–26], NMC [27–31], SLAC [32] and E665 [33, 34] Collaborations. The measured nuclear targets involved into our analysis are listed in Table 1. These data make the total of 333 points. To estimate the nucleus radius we use well-known parametrization applied earlier [22] and another one [54], namely

$$R_A = (1.12A^{1/3} - 0.86A^{-1/3}) \text{ fm}, \quad (12)$$

and

$$R_A = (1.12A^{1/3} - 0.5) \text{ fm}. \quad (13)$$

The latter formula may have an advantage of a better agreement with the proton radius  $R_p \sim 0.7$  fm obtained from fits based on the scaling approach [22]. Below we denote the fit obtained with (12) as 'Fit I' and with (13) as 'Fit II'. Note that we take the deuteron to be identical to the proton, so that  $R_D = R_p$  and  $A_D = 1$ .

Our fits for  $\pi R_p^2$  and  $\delta$  parameters lead to  $\pi R_p^2 = 1.74 \pm 0.20 \text{ fm}^2$ ,  $\delta = 0.751 \pm 0.026$  with  $\chi^2/n.d.f. = 2.28$  for Fit I and  $\pi R_p^2 = 1.86 \pm 0.20 \text{ fm}^2$ ,  $\delta = 0.740_{-0.021}^{+0.041}$  with  $\chi^2/n.d.f. = 2.19$  for Fit II. The experimental data involved into the fit procedures are compared with our predictions in Fig. 1. It can be seen that the both fits allow to describe the various data quite well. Some systematic underestimation can be seen for E665 data on  $F_2^{\text{Pb}}/F_2^{\text{D}}$ ,  $F_2^{\text{Ca}}/F_2^{\text{D}}$  and  $F_2^{\text{C}}/F_2^{\text{D}}$ , which, however, does not exceed two standard deviations at any point. Another source of discrepancy comes from NMC data on  $F_2^{\text{Sn}}/F_2^{\text{C}}$ . We find that Fit II leads to somewhat better agreement with the data, especially the data on light nuclei ( $^4\text{He}$ ,  $^6\text{Li}$ ,  $^{12}\text{C}$ ) at low  $x$ , that is an immediate consequence of closer limit  $R_A \rightarrow R_p \sim 0.7$  fm for small  $A$  achieved with (13). Note that for the most of the used data the points are taken for different  $Q^2$ , so one should consider the lines depicted in Fig. 1 as interpolations in both  $x$  and  $Q^2$ .

In Fig. 2 we present results for effective (integrated over  $\mathbf{k}_T^2$  up to scale  $\mu^2$ ) nuclear gluon distribution functions  $xg^A(x, \mu^2)$  divided by  $A$  for several nuclei as functions of the momentum fraction  $x$  in the region of the fit,  $x \leq 0.1$ . Such quantities, in principle, could be compared with ordinary nPDFs (see discussion below). The upper limit of the integration is chosen to be equal to  $\mu^2 = Q_0^2$ , where  $Q_0$  is the starting scale of subsequent QCD evolution applied to the LLM gluon density (7), see [20]. Our choice is motivated by the fact that all phenomenological parameters involved in (7) were determined up to this scale. Shaded bands represent the estimated uncertainties of our fit procedure. As one can see, the difference between the Fit I and Fit II appears mainly at low  $x$  and is more pronounced for heavier nuclei. The obtained results can be compared with predictions [22, 38], which are based on the GBW form of the gluon density (6). So, the ansatz (9) was applied in the calculations [22] and another condition, namely,  $Q_{s,A}^2(x) = A^{1/3}Q_s^2(x)$ , was also tested [38]. We label these predictions as nGBW (A) and nGBW (B), respectively (see Fig. 2). Note that in the nGBW (A) analysis, the nuclear radius  $R_A$  is given by (12) and free parameters  $\delta = 0.79 \pm 0.02$  and  $\pi R_p^2 = 1.55 \pm 0.02 \text{ fm}^2$  were determined [22] from experimental data on  $\gamma^*A$  collisions. In the nGBW (B) calculations, the additional relation

$R_A/R_p = A^{1/3}$  is assumed. Despite the similar values of phenomenological parameters  $\delta$  and  $\pi R_p^2$  obtained in both our fits and nGBW (A) analysis, we find a notable difference between the corresponding predictions for effective nuclear gluon densities. Moreover, the nGBW (A) and nGBW (B) results also differ from each other. It is explained, of course, by the distinctions in the theoretical input used in these calculations<sup>5</sup>. In fact, while an  $A$ -dependence of  $Q_{s,A}^2(x) \sim A^{1/3}$ , implemented into the nGBW (B) calculations, is often assumed, there are approaches where much stronger,  $Q_{s,A}^2(x) \sim A^{2/3}$ , weaker,  $Q_{s,A}^2(x) \sim A^\alpha$  with  $\alpha \ll 1/3$ , or even logarithmic  $A$ -dependencies are favored (see, for example, [7, 55–59] and references therein).

In addition, we plot here nPDFs obtained by the nCTEQ Collaboration [7] and based on the global fit to nuclear data in the framework of the DGLAP evolution scenario. It also shows many differences with the approaches discussed above. However, we point out that direct comparison between the effective ( $\mathbf{k}_T^2$ -integrated) nTMDs and conventional nPDFs can only be approximate since these quantities are essentially different objects. In fact, there is no obvious resummation of any type of large logarithmic terms in the modelled TMD gluon densities (6) or (7).

Now we turn to the discussion of the nuclear shadowing effects in the gluon distributions at low  $x$ . As usual, we consider the nuclear modification factor for light and heavy nuclei defined as a ratio  $R_g^A(x, \mu^2) = (1/A)xg^A(x, \mu^2)/xg(x, \mu^2)$ . The results of our calculations are shown in Fig. 3. These calculations have been done at  $\mu^2 = Q_0^2$ , which approximately corresponds to the kinematical regime of experiments [23–34] performed by the EMC, NMC, SLAC and E665 Collaborations at  $x < 0.1$ . Exact value of  $\mu^2$  is not important here since the scale dependence of nuclear modification factor  $R_g^A(x, \mu^2)$  at low  $\mu^2$  is almost negligible. As it was expected, we observe that both our fits results in a sizeable gluon shadowing. This effect becomes more important with decreasing of  $x$  and increasing of  $A$ . Nevertheless, the nuclear modification in all the considered approaches shows some difference. So, in our calculations using Fit I it is a little weaker in comparison with predictions of Fit II. The shadowing magnitude obtained in the nGBW (A)/(B) calculations at low  $x$  is a bit smaller/larger than both of our results, respectively. At the same time, predictions of Fit I and Fit II at low  $x \leq 10^{-4}$  are typically a bit stronger for all nuclei than that of global analyses performed by the nCTEQ [7] or nIMP [8] groups within the DGLAP framework. Around  $x \sim 10^{-3}$ , our results are rather close to them. At larger  $x$ , there is some gluon anti-shadowing effect, which is observed in both Fit I and Fit II scenarios. This effect is an interesting feature and clearly seen also in the nGBW (A) and nCTEQ calculations. In contrast, it is practically absent in the nGBW (B) and nIMP analyses. Such difference in predictions of these approaches is notable and shows the importance of studying the gluon nuclear modification factor in future experiments. In the applied approach, this factor depends on the exact way of the transformation of the saturation scale in nucleus (see [22]). We stress that in our fits the form of such modification and corresponding parameters come from the best description of the data on the nuclear structure functions  $F_2^A(x, Q^2)$ . Indeed, more experimental data are needed to distinguish between the different nPDF models.

To conclude, the main outcome of the present study is new TMD gluon densities in a nucleus. We extend the previously proposed TMD gluon density in a proton to nuclei using the well established empirical property of geometric scaling. It modifies the gluon saturation scale  $Q_s(x)$  in a way to incorporate nuclear medium effects leading to shadowing of gluon distributions at small  $x$ . It is important that, in contrast with other studies, the input gluon density in a proton applied in our analysis is able to reproduce a number of HERA and LHC data, that is an advantage of our consideration. The

---

<sup>5</sup>We successfully recover the results [38], where nGBW (B) scenario was applied.

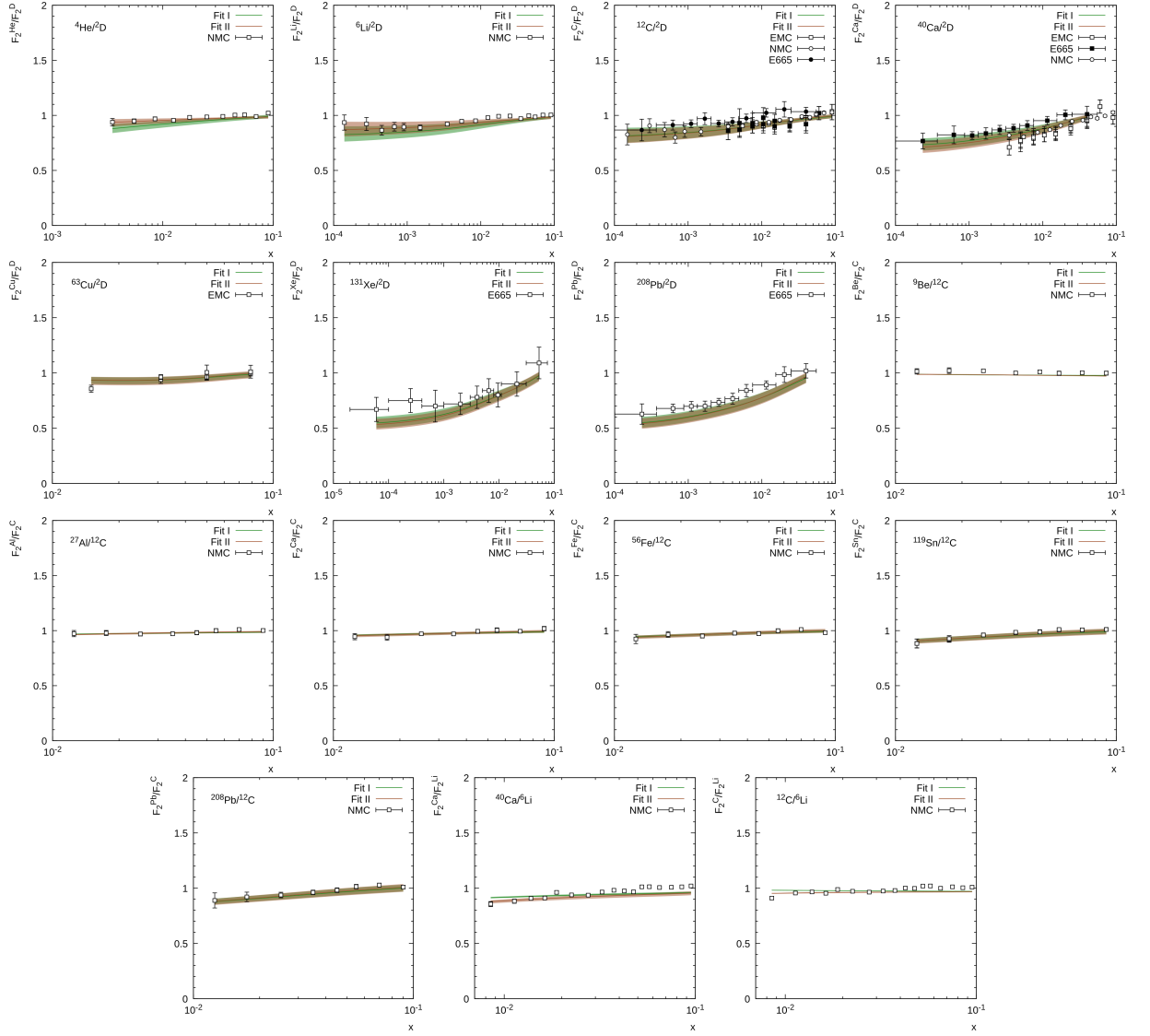


Figure 1: The global fit results of structure function ratios  $F_2^A(x, Q^2)/F_2^{A'}(x, Q^2)$  between different nuclei targets  $A$  and  $A'$ . Shaded bands represent the estimated uncertainties of our fit procedure. Experimental data are from NMC [27–31], EMC [23–26], SLAC [32] and E665 [33, 34].

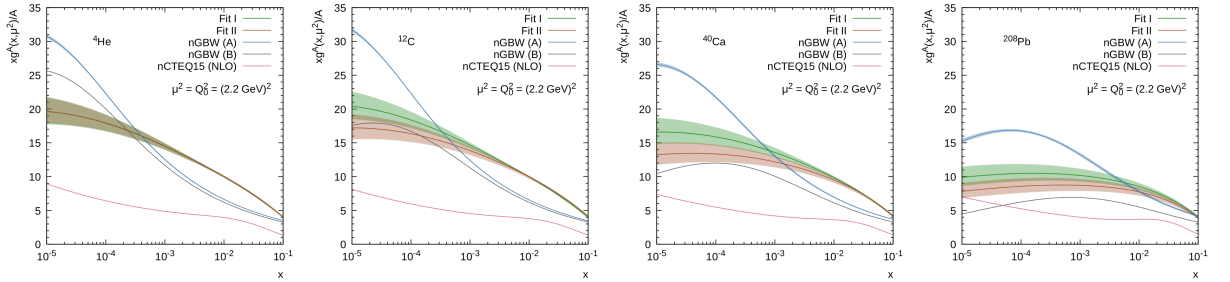


Figure 2: Effective (integrated over  $\mathbf{k}_T^2$ ) gluon densities in some light and heavy nuclei (namely,  $^4\text{He}$ ,  $^{12}\text{C}$ ,  $^{40}\text{Ca}$  and  $^{208}\text{Pb}$ ) calculated as functions of  $x$  at  $\mu^2 = Q_0^2$ . For comparison we show here corresponding nPDFs obtained by the nCTEQ Collaboration [7].



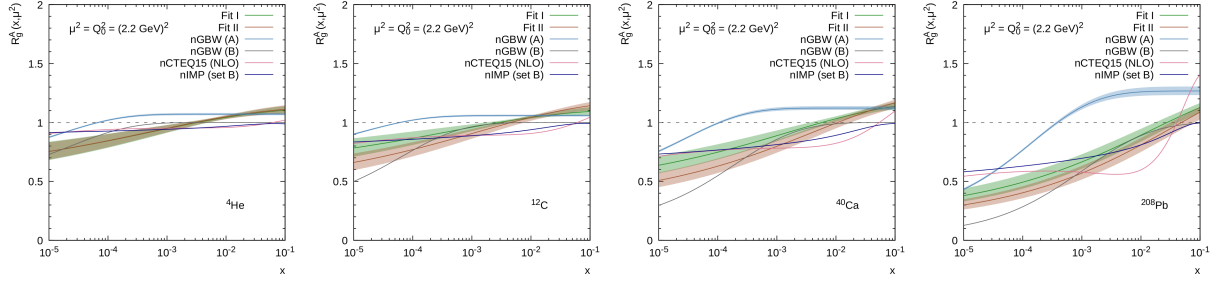


Figure 3: Nuclear modification factor for gluon densities in some light and heavy nuclei (namely,  $^4\text{He}$ ,  $^{12}\text{C}$ ,  $^{40}\text{Ca}$  and  $^{208}\text{Pb}$ ) calculated as functions of  $x$  at  $\mu^2 = Q_0^2$ . For comparison we show here corresponding results obtained by the nCTEQ [7] and nIMP [8] groups.

parameters of the scale modification have been obtained from a fit to various data on ratios  $F_2^A(x, Q^2)/F_2^{A'}(x, Q^2)$  for several nuclear targets at low  $x < 0.1$ . The latter have been calculated using the color dipole formalism. Two fits relying on different formulae for the nuclear radius have been performed and both of them provide reasonable description of the data. So, we have shown that one can include the shadowing effect in nuclei collisions by the modification of the saturation scale and demonstrate that the developed approach can be applied in the phenomenological studies in the shadowing region within the dipole formalism. Moreover, our fits could be used also as an initial condition for the subsequent non-collinear QCD evolution. It is important for future studies of lepton-nucleus, proton-nucleus and nucleus-nucleus interactions at modern and future colliders, where the gluon saturation dynamics could be examined directly.

*Acknowledgements.* We thank S.P. Baranov and H. Jung for their interest, very important comments and remarks. This research has been carried out at the expense of the Russian Science Foundation grant No. 25-22-00066, <https://rscf.ru/en/project/25-22-00066/>.

## References

- [1] EMC Collaboration, Phys. Lett. B **123**, 275 (1983).
- [2] M. Arneodo, Phys. Rept. **240**, 301 (1994).
- [3] P.R. Norton, Rept. Prog. Phys. **66**, 1253 (2003).
- [4] S. Malace, D. Gaskell, D.W. Higinbotham, I.C. Clöt, Int. J. Mod. Phys. E **23**, 1430013 (2014).
- [5] K.J. Eskola, P. Paakkinen, H. Paukkunen, C.A. Salgado, Eur. Phys. J. C **82**, 413 (2022).
- [6] R.A. Khalek, R. Gauld, T. Giani, E.R. Nocera, T.R. Rabemananjara, J. Rojo, Eur. Phys. J. C **82**, 507 (2022).
- [7] A.W. Denniston, T. Jezo, A. Kusina, N. Derakhshanian, P. Duwentaster, O. Hen, C. Keppel, M. Klasen, K. Kovarik, J.G. Morfin, K.F. Muzakka, F.I. Olness, E. Pisasetzky, P. Risse, R. Ruiz, I. Schienbein, J.Y. Yu, Phys. Rev. Lett. **133**, 152502 (2024).
- [8] R. Wang, X. Chen, Q. Fu, Nucl. Phys. B **920**, 1 (2017).

- [9] S.A. Kulagin, R. Petti, Nucl. Phys. A **765**, 126 (2006).
- [10] S.A. Kulagin, R. Petti, Phys. Rev. C **90**, 045204 (2014).
- [11] M. Hirai, S. Kumano, T.-H. Nagai, Phys. Rev. C **70**, 04495 (2004).
- [12] M. Hirai, S. Kumano, T.-H. Nagai, Phys. Rev. C **76**, 065207 (2007).
- [13] K.J. Eskola, Nucl. Phys. A **910**, 163 (2013).
- [14] J.C. Collins, D.E. Soper, Nucl. Phys. B **194**, 445 (1982);  
J.C. Collins, D.E. Soper, Nucl. Phys. B **197**, 446 (1982);  
J.C. Collins, D.E. Soper, G.F. Sterman, Nucl. Phys. B **223**, 381 (1983);  
J.C. Collins, D.E. Soper, G.F. Sterman, Nucl. Phys. B **250**, 199 (1985).
- [15] S. Catani, M. Ciafaloni, F. Hautmann, Nucl. Phys. B **366**, 135 (1991);  
J.C. Collins, R.K. Ellis, Nucl. Phys. B **360**, 3 (1991).
- [16] L.V. Gribov, E.M. Levin, M.G. Ryskin, Phys. Rep. **100**, 1 (1983);  
E.M. Levin, M.G. Ryskin, Yu.M. Shabelsky, A.G. Shuvaev, Sov. J. Nucl. Phys. **53**, 657 (1991).
- [17] R. Angeles-Martinez, A. Bacchetta, I.I. Balitsky, D. Boer, M. Boglione, R. Boussarie, F.A. Ceccopieri, I.O. Cherednikov, P. Connor, M.G. Echevarria, G. Ferrera, J. Grados Luyando, F. Hautmann, H. Jung, T. Kasemets, K. Kutak, J.P. Lansberg, A. Lelek, G.I. Lykasov, J.D. Madrigal Martinez, P.J. Mulders, E.R. Nocera, E. Petreska, C. Pisano, R. Placakyte, V. Radescu, M. Radici, G. Schnell, I. Scimemi, A. Signori, L. Szymanowski, S. Taheri Monfared, F.F. Van der Veken, H.J. van Haevermaet, P. Van Mechelen, A.A. Vladimirov, S. Wallon, Acta Phys. Polon. B **46**, 2501 (2015).
- [18] A.V. Lipatov, S.P. Baranov, M.A. Malyshev, Phys. Part. Nucl. **55**, 256 (2024).
- [19] A.V. Lipatov, G.I. Lykasov, M.A. Malyshev, Phys. Rev. D **107**, 014022 (2023).
- [20] A.V. Lipatov, G.I. Lykasov, M.A. Malyshev, JETP Lett. **119**, 828 (2024).
- [21] A.M. Stasto, K. Golec-Biernat, J. Kwiecinski, Phys. Rev. Lett. **86**, 596 (2001).
- [22] N. Armesto, C.A. Salgado, U.A. Wiedemann, Phys. Rev. Lett. **94**, 022002 (2005).
- [23] European Muon Collaboration, Phys. Lett. B **202**, 603 (1988).
- [24] European Muon Collaboration, Phys. Lett. B **211**, 493 (1988).
- [25] European Muon Collaboration, Nucl. Phys. B **333**, 1 (1990).
- [26] European Muon Collaboration, Z. Phys. C **57**, 211 (1993).
- [27] New Muon Collaboration, Z. Phys. C **53**, 73 (1992).
- [28] New Muon Collaboration, Nucl. Phys. B **441**, 3 (1995).
- [29] New Muon Collaboration, Nucl. Phys. B **441**, 12 (1995).
- [30] New Muon Collaboration, Nucl. Phys. B **481**, 3 (1996).
- [31] New Muon Collaboration, Nucl. Phys. B **481**, 23 (1996).

- [32] J. Gomes et al., Phys. Rev. D **49**, 4348 (1994).
- [33] Fermilab E665 Collaboration, Phys. Rev. Lett. **68**, 3266 (1992).
- [34] Fermilab E665 Collaboration, Z. Phys. C **67**, 403 (1995).
- [35] A.V. Lipatov, G.I. Lykasov, M.A. Malyshev, Phys. Lett. B **839**, 137780 (2023).
- [36] A.V. Lipatov, M.A. Malyshev, Phys. Rev. D **108**, 014022 (2023).
- [37] A.V. Lipatov, G.I. Lykasov, M.A. Malyshev, Phys. Lett. B **848**, 138390 (2024).
- [38] G.R. Boroun, B. Rezaei, Pramana J. Phys. **98**, 161 (2024).
- [39] K. Golec-Biernat, M. Wüsthoff, Phys. Rev. D **59**, 014017 (1998).
- [40] K. Golec-Biernat, M. Wüsthoff, Phys. Rev. D **60**, 114023 (1999).
- [41] K. Golec-Biernat, L. Motyka, T. Stebel, Phys. Rev. D **103**, 034013 (2021).
- [42] L.L. Frankfurt, M.I. Strikman, Phys. Rept. **160**, 235 (1988).
- [43] A.H. Mueller, Nucl. Phys. B **335**, 115 (1990).
- [44] N.N. Nikolaev, B.G. Zakharov, Z. Phys. C **49**, 607 (1991).
- [45] N.N. Nikolaev, B.G. Zakharov, Phys. Lett. B **332**, 184 (1994).
- [46] N.N. Nikolaev, B.G. Zakharov, Z. Phys. C **64**, 631 (1994).
- [47] J. Bartels, K. Golec-Biernat, H. Kowalski, Phys. Rev. D **66**, 014001 (2002).
- [48] A.M. Snigirev, G.M. Zinovjev, Phys. Rev. D **100**, 094008 (2019).
- [49] M. Ciafaloni, Nucl. Phys. B **296**, 49 (1988);  
S. Catani, F. Fiorani, G. Marchesini, Phys. Lett. B **234**, 339 (1990);  
S. Catani, F. Fiorani, G. Marchesini, Nucl. Phys. B **336**, 18 (1990);  
G. Marchesini, Nucl. Phys. B **445**, 49 (1995).
- [50] I. Balitsky, Nucl. Phys. B **463**, 99 (1996);  
Y.V. Kovchegov, Phys. Rev. D **60**, 034008 (1999).
- [51] N. Armesto, M.A. Braun, Eur. Phys. J. C **20**, 517 (2001).
- [52] M. Lublinsky, Eur. Phys. J. C **21**, 513 (2001).
- [53] S. Munier, R. Peschanski, Phys. Rev. Lett. **91**, 232001 (2003).
- [54] I.M. Kapitonov, "An Introduction to Physics of Nuclei and Particles",  
URSS, Moscow, 2002.
- [55] L.D. McLerran, R. Venugopalan, Phys. Rev. D **49**, 2233 (1994);  
L.D. McLerran, R. Venugopalan, Phys. Rev. D **49**, 3352 (1994).
- [56] A.H. Mueller, Nucl. Phys. A **724**, 223 (2003).
- [57] K. Rummukainen, H. Weigert, Nucl. Phys. A **739**, 183 (2004).
- [58] Y.V. Kovchegov, Phys. Rev. D **61**, 074018 (2000).
- [59] E. Levin, K. Tuchin, Nucl. Phys. B **573**, 833 (2000).